ELSEVIER

Journal of Organometallic Chemistry 524 (1996) 71–80

Journal of Organometallic Chemistry

Regioselectivity in the nucleophilic functionalization of dibenzofuran, dibenzothiophene and xanthene complexes of $Mn(CO)_3^+$

Ivana Verona [a], James P. Gutheil [a], Robert D. Pike [a,*], Gene B. Carpenter [b]

[a] *Department of Chemistry, College of William and Mary, Williamsburg, VA 23187, USA*
[b] *Department of Chemistry, Brown University, Providence, RI 02912, USA*

Received 24 January 1996; revised 11 March 1996

Abstract

The cationic complexes $[(\eta^6\text{-DBF})Mn(CO)_3]BF_4$, $[(\eta^6\text{-DBT})Mn(CO)_3]BF_4$ and $[(\eta^6\text{-XAN})Mn(CO)_3]PF_6$ (DBF = dibenzofuran, DBT = dibenzothiophene, XAN = xanthene) are prepared. These species react with carbon-based nucleophiles to form exo-substituted cyclohexadienyl complexes. Addition is found exclusively at carbons 1 and 4. The C(1)-functionalized regioisomer predominates, especially for the DBF and XAN complexes, for which 90 to > 95% selectivity is found with stabilized nucleophiles. Preference for C(1) is greatly reduced for unstabilized magnesium and lithium nucleophiles. The origin of this selectivity is discussed. Loss of the aromatic ring from the cationic complexes in the presence of CH_3CN is found to be extremely facile for the DBF and DBT complexes owing to increased ease of ring slippage. Second-order rate constants for the displacement reactions with CH_3CN are $4.6 \pm 0.6 \times 10^{-5}\ M^{-1}\ s^{-1}$ (DBF complex, 25 °C), $4.4 \pm 1.0 \times 10^{-5}\ M^{-1}\ s^{-1}$ (DBT complex, 25 °C) and about $1.0 \times 10^{-5}\ M^{-1}\ s^{-1}$ (XAN complex, 60 °C). A crystal structure is presented for the hydride adduct of the DBF complex, $[(\eta^5\text{-}C_{12}H_9O)Mn(CO)_3]$: space group $P2_1/c$, $a = 15.301(2)$, $b = 6.4422(12)$, $c = 12.988(2)$ Å, $\beta = 90.888(13)°$, $V = 1280.1(3)$ Å^3, $Z = 4$, $D_{calc} = 1.599\ Mg\ m^{-3}$, $R = 0.0410$ and $wR2 = 0.0945$ on 2446 reflections with $F^2 > 4.0\sigma(F^2)$.

Keywords: Manganese; Arene complexes; Nucleophilic addition; Heterocycles

1. Introduction

The coordination of aromatic molecules to electron-deficient metal fragments has proved to be an effective method of activation toward nucleophilic attack [1]. Typically, (η^6-arene)metal complexes have been found to react with carbon nucleophiles at the aromatic ring to produce (η^5-cyclohexadienyl)metal species. In particular, the $[Mn(CO)_3]^+$ fragment [2] imparts far greater reactivity to coordinated arenes than do the isoelectronic $[FeCp]^+$ or $[Cr(CO)_3]$ fragments. Previous addition reactions of the manganese [3–5] and other [6] arene complexes have shown a relatively low degree of regioselectivity, yielding a mixture of substitutional isomers upon decomplexation (Scheme 1). The principal directing effect for $[(\eta^6\text{-arene})Mn(CO)_3]^+$ appears to be that of ether and amine substituents toward the *meta* position. In the case of aromatic ethers, the regiochemical preference for attack at the *meta* position has been exploited in the synthesis of natural product, antibiotic and anti-inflammatory compounds [7].

There has been relatively little investigation of nucleophilic addition to fused ring heterocyclic complexes of $[Mn(CO)_3]^+$. Sweigart and coworkers have prepared η^6-complexes of benzofuran and several N-substituted indoles [8]. Nucleophilic addition to these cations afforded products **1**:**2** or **3**:**4** in ratios of 0.5–3:1, except when the indole nitrogen substituent R′ was the very bulky $SiPh_2{}^tBu$ or Si^iPr_3.

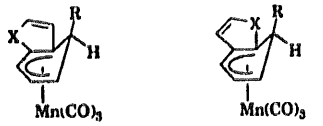

1: X = NR′ **2**: X = NR′
3: X = O **4**: X = O

* Corresponding author.

PII S0022-328X(96)06347-4

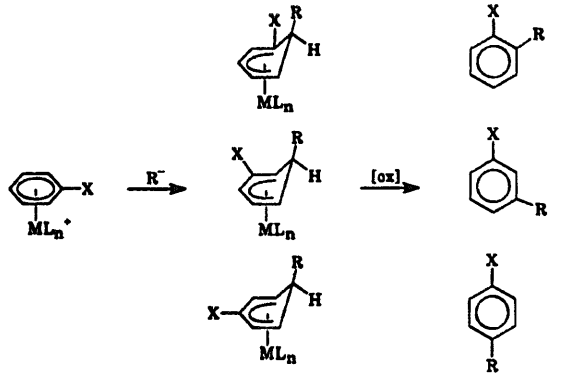

Scheme 1.

Herein, we present some results of carbanion addition to the $[Mn(CO)_3]^+$ complexes of dibenzofuran (DBF, **5**), dibenzothiophene (DBT, **6**) and xanthene (XAN, **7**).

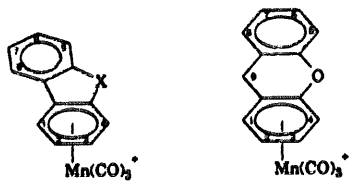

5: X = O
6: X = S

7

2. Results

2.1. Nucleophilic addition reactions of 5–7

We recently reported the synthesis of η^6-fused ring complexes **5** [9] and **6** [10] as their BF_4^- salts. Both species are produced in good yield by the reaction of $[Mn_2(CO)_{10}]$ with the arene in refluxing trifluoroacetic anhydride with aqueous HBF_4 [10]. When the xanthene complex, **7**, is prepared by this method, yields are somewhat low. This appears to be due to the oxidation of xanthene to the fully aromatic xanthylium cation. A better product yield of 60% was obtained under Fischer–Hafner conditions [10]. Like other $[(\eta^6\text{-arene})Mn(CO)_3]^+$ compounds, **5–7** are stable to air and moisture. Complexes exhibiting the η^6-coordination mode of DBF, DBT and/or XAN are known for several other 12-electron metal fragments, including $[Cr(CO)_3]$ [11], $[FeCp]^+$ [12], $[RuCp]^+$ [13], and $[Ir(COD)]^+$ [14]. Unlike the prior examples of η^6-DBF, -DBT and -XAN complexation, the $[Mn(CO)_3]^+$ fragment was found to produce a sharp downfield shift in the ^1H NMR resonances for the coordinated ring. This is probably the result of the extreme electron-withdrawing ability of the manganese fragment, producing a large resonance deshielding effect. The electron-deficiency of the manganese-coordinated fused ring heterocycles was further evident in the reactivity of these complexes toward both mild carbanions and neutral donor solvents.

The reactions of **5**, **6** and **7** with hydride and a variety of carbanions were carried out. The synthetic conditions and results are shown in Table 1. The addition reactions were quite rapid, most being complete within 1 h at 0 or −78 °C. Most of the reactions were accompanied by a color change from yellow to orange and by increased solubility. The reactions could also be followed by IR. The carbonyl bands underwent a shift from about 2078, 2020 cm^{-1} for the arene cations to about 2020, 1945 cm^{-1} for the cyclohexadienyl products. In all cases shown, the reaction proceeded smoothly

Table 1
Results of nucleophile addition to **5**, **6** and **7**

Product	Nucleophile	Solvent, Temp.(°C)	Total yield (%)	Isomer ratio	ν_{CO} [a] (cm^{-1})
8a/9a	$NaBH_4$	THF, 25	93	14:1	2022, 1952, 1942
8b/9b	MgBrPh	CH_2Cl_2, 0	88	11:1	2022, 1952, 1944
8b/9b	LiPh	CH_2Cl_2, −78	71	12:1	2020, 1953, 1943
8c/9c	LiC_2Ph	Et_2O, −78	83	11:1	2024, 1954, 1946
8d/9d	$MgClCH_2Ph$ [b]	CH_2Cl_2, 0	55	6:1	2022, 1951, 1942
8e/9e	$MgClCHMe_2$	CH_2Cl_2, 0 [c]	62	1.5:1	2020, 1949, 1940
8f/9f	$MgBrCH_2CH_3$	CH_2Cl_2, 0	45	3:1	2020, 1949, 1941
10a/11a	$NaBH_4$	THF, 25	84	2:1	2018, 1947, 1940
10b/11b	MgBrPh	Et_2O, 0	77	3:1	2020, 1950, 1938
10b/11b	LiPh	CH_2Cl_2, −78	70	3:1	2020, 1952, 1942
10c/11c	LiC_2Ph	Et_2O, −78	72	2:1	2021, 1952, 1944
10d/11d	$MgClCH_2Ph$ [b]	Et_2O, 0	60	1:1	2020, 1950, 1940
12a [d]	$NaBH_4$	THF, 25	78	—	2020, 1943(br)
12b [d]	MgBrPh	CH_2Cl_2, 0	95	—	2019, 1945, 1942
12b [d]	LiPh	CH_2Cl_2, −78	70	—	2021, 1945, 1943
12c [d]	LiC_2Ph	Et_2O, −78	40	—	2023, 1948, 1946
12d/13d	$MgClCH_2Ph$	CH_2Cl_2, 0	100	3.3:1	2020, 1944(br)
12e/13e	$MgClCHMe_2$	CH_2Cl_2, 0	62	1.7:1	2020, 1943(br)

[a] In C_6H_{14}; all band intensities strong. [b] $MgBrCH_2Ph$ gave similar results. [c] Reaction in Et_2O at 0 °C gave similar results. [d] Isomer **13** not observed.

Table 2
Analysis data for selected complexes 8–13

Complex	Calc.	Found
8b/9b	C 65.64	C 65.68
	H 3.41	H 3.83
8d/9d	C 66.34	C 65.53
	H 3.80	H 4.10
10a/11a	C 55.57	C 55.51
	H 2.80	H 3.17
10b/11b	C 63.91	C 63.97
	H 3.27	H 3.62
10c/11c	C 65.10	C 66.82
	H 3.09	H 3.41
12a	C 59.64	C 59.64
	H 3.44	H 3.59
12e/13e	C 62.65	C 61.23
	H 4.70	H 4.80

and the products were readily isolated after destruction of excess nucleophile and extraction into a non-polar solvent.

As shown in Scheme 2, the nucleophile additions yielded mixtures containing only two regioisomers. Dichloromethane and diethyl ether were used interchangeably throughout the study. The effects of these solvents and of tetrahydrofuran (THF) were examined during the synthesis of **8e/9e**. Ether and CH_2Cl_2 were found to result in identical yields and isomer ratios. (A very small amount of what may be a third regioisomer was identified in the ^1H NMR of **8e/9e** which was prepared in diethyl ether.) In contrast, THF was found to be a poor solvent for the Grignard reaction. Free DBF was recovered, rather than the desired **8e/9e**. Since THF is a coordinating solvent, it presumably promotes solvolysis of the labile arene (vide infra). It is interesting that THF did not interfere with the reaction of $NaBH_4$. The effect of Grignard source on regioselectivity was studied by preparing products **8d/9d** and **10d/11d** using $MgXCH_2Ph$ (X = Cl or Br) at 0°C in CH_2Cl_2. Isomer ratios were found to be independent of Grignard source.

Table 3
^1H NMR data for complexes 8 and 9 [a]

	8a/9a	8b/9b	8c/9c	8d/9d	8e/9e	8f/9f
H(5–8), H(Ph)	7.7 (m)	7.4 (m)	7.6 (m)	7.6 (m)	7.6 (m)	7.6 (m)
H(4)	6.50 (d, 5.7)	6.43 (d, 5.8)	6.42 (d, 5.7)	6.24 (d, 5.7)	6.30 (d, 6.0)	6.31 (d, 5.1)
H(3)	4.99 (t, 6.5)	5.02 (t, 6.4)	4.97 (t, 6.4)	4.85 (t, 6.4)	4.90 (t, 6.6)	4.85 (t, 5.3)
H(2)	3.18 (t, 6.3)	3.58 (t, 6.4)	3.39 (t, 6.2)	3.16 (t, 6.2)	3.24 (t, 6.4)	3.26 (t, 6.2)
H(1-endo)	3.70 (dd, 13.5, 6.7)	4.96 (d, 5.3)	4.67 (d, 5.3)	3.89 (q, 6.0)	3.46 (t, 6.2)	3.56 (q, 6.2)
H(1')	6.39 (d, 4.7)	6.34 (d, 5.3)	6.37 (d, 5.7)	6.12 (d, 5.3)	6.18 (d, 4.8)	6.21 (d, 4.8)
H(2')	4.94 (t, 7.5)	5.00 [b]	4.90 (t, 5.3)	4.77 (t, 6.2)	4.84 (t, 6.4)	4.80 (d, 6.4)
H(3')	3.30 (t, 6.5)	3.69 (t, 5.7)	3.51 (t, 5.7)	3.21 (t, 6.2)	3.35 (t, 6.4)	3.36 (t, 6.4)
H(4'-endo)	3.93 (dd, 13.8, 5.6)	5.19 (d, 6.2)	4.67 (d, 5.3)	4.14 (dt, 5.3, 4.6)	3.71 (t, 6.2)	3.80 (q, 5.3)
Others	2.61 (d, 13.5, H(1-exo)); 2.97 (d, 13.8, H(1'-exo))	—	—	1.98 (m, CH_2); 2.33 (m, CH'_2)	0.85 (m, CH); 0.53 (m, CH_3); 0.98 (m, CH'); 0.42 (m, CH'_3)	0.70 (m, CH_2); 0.49 (t, 7.5, CH_3); 1.35 (m, CH'_2); 0.88 (t, 7.0, CH'_3)

[a] In $CDCl_3$; coupling constant J (Hz) values in parentheses. Prime designations refer to minor isomer, 9; see Schemes 1–3 and 2 for numbering.
[b] Coupling obscured by peak overlap.

Table 4
^1H NMR data for complexes 10 and 11 [a]

	10a/11a	10b/11b	10c/11c	10d/11d
H(5–8), H(Ph)	7.7 (m)	7.5 (m)	7.5 (m)	7.5 (m)
H(4)	6.59 (d, 5.2)	6.54 (d, 5.3)	6.51 (d, 5.7)	6.37 (d, 5.3)
H(3)	5.12 (t, 6.2)	4.90 (t, 6.2)	5.13 (t, 6.4)	5.05 (t, 6.4)
H(2)	3.23 (t, 6.3)	3.51 (t, 6.4)	3.45 (t, 6.2)	3.25 (t, 6.2)
H(1-endo)	3.74 (dd, 13.5, 6.0)	4.75 (d, 5.5)	4.65 (d, 5.7)	3.99 (m)
H(1')	6.68 (d, 5.2)	6.59 (d, 5.2)	6.60 (d, 5.3)	6.50 (d, 5.3)
H(2')	5.09 (t, 6.0)	4.93 (t, 6.2)	5.06 (t, 6.4)	4.99 (t, 6.4)
H(3')	3.31 (t, 6.3)	3.53 (t, 6.3)	3.52 (t, 6.2)	3.25 (t, 6.2)
H(4'-endo)	3.70 (dd, 13.7, 5.5)	4.85 [b]	4.71 (d, 5.7)	3.99 (m)
Others	2.53 (d, 13.4, H(1-exo)); 2.84 (d, 13.7, H(1'-exo))	—	—	2.11 (dd, 13.2, 4.8 CH_2); 1.91 (m, CH_2); 2.41 (dd, 13.0, 4.6 CH'_2); 1.98 (m, CH'_2)

[a] In $CDCl_3$; coupling constant J (Hz) values in parentheses. Prime designations refer to minor isomer, 11; see Schemes 4 for numbering.
[b] Coupling obscured by peak overlap.

Table 5
^{1}H NMR data for complexes **12** and **13** [a]

	12a	12b	12c	12d/13d	12e/13e
H(5–8), H(Ph)	7.0 (m)	7.0 (m)	7.1 (m)	7.1 (m)	7.1 (m)
H(4)	5.90 (d, 5.3)	5.85 (d, 5.3)	5.94 (d, 5.3)	5.88 (d, 5.7)	5.82 (d, 5.7)
H(3)	4.84 (t, 6.2)	4.91 (m)	4.96 (t, 6.4)	4.88 (t, 6.8)	4.91 (t, 5.3)
H(2)	2.80 (t, 6.3)	3.88 (t, 5.9)	3.13 (t, 6.4)	2.92 (m)	3.04 (t, 6.4)
H(1-endo)	2.63 (dd, 5.9, 13.0)	4.91 (m)	3.64 (d, 5.7)	2.92 (m)	2.65 (t, 5.7)
H(9)	3.20 (m)	3.30 (m)	3.50 (m)	3.34 (m)	3.30 (m)
H(1′)	—	—	—	5.19 (d, 4.9)	5.28 (d, 5.3)
H(2′)	—	—	—	4.73 (t, 6.5)	4.78 (t, 5.9)
H(3′)	—	—	—	3.09 (t, 5.7)	2.96 (t, 6.6)
H(4′-endo)	—	—	—	3.47 (m)	2.23 (t, 6.6)
H(9′)	—	—	—	3.82 (m)	3.30 (m)
Others	2.38 (d, 12.7,H (1-exo))	—	—	2.38 (dd, 9.0, 4.0, CH_2), 1.98 (dd, 12.7, 8.0, CH_2), 2.57 (dd, 12.7, 4.0, CH'_2), 2.15 (dd, 13.0, 8.6, CH'_2)	1.26 (m, CH); 1.16 (m, CH′); 0.72 (m, CH_3, CH'_3)

[a] In $CDCl_3$; coupling constant J (Hz) values in parentheses. Prime designations refer to minor isomer, **13**; see Schemes 5 for numbering.

The (cyclohexadienyl)manganese products **8–13** were air-stable orange solids or oils. Spectral and analytical data for these species are given in Table 6. Although the mixtures were found to be separable via chromatography on silica gel with hexane eluant, all of the isomeric ratios listed in Table 1 were determined by ^{1}H NMR integration. The regiochemistry of addition was determined by full proton–proton decoupling of each spec-

Table 6
^{13}C{^{1}H} NMR data for complexes **8–13**

Complex	^{13}C NMR [a]
8a	223, 156.7, 136.9, 129.2, 126.7, 123.9, 120.4, 111.5, 92.7, 68.4, 62.7, 51.9, 26.7 [b]
8b	222, 150.2, 144.5, 128.8, 128.2, 127.7, 126.6, 126.3, 125.5, 124.1, 117.5, 116.8, 92.1, 76.8, 68.0, 57.1, 48.5, 44.2, 27.9 [b]
8c	222, 132.8, 131.9, 128.7, 128.3, 128.0, 127.8, 127.4, 127.1, 124.2, 123.1, 123.0, 120.9, 120.6, 112.0, 111.7, 91.0, 63.8, 54.6, 29.4, 1.2 [b]
8d	222, 156.5, 137.5, 136.3, 129.5, 128.9, 128.5, 126.5, 126.2, 123.8, 123.0, 120.2, 111.4, 91.2, 73.2, 63.2, 56.5, 48.0, 40.7, 38.2 [b]
8e/9e	224, 159.9, 156.6, 137.4, 130.4, 129.5, 128.2, 127.1, 124.9, 124.7, 124.5, 123.7, 122.0, 121.6, 112.8, 112.3, 111.9, 94.7, 92.7, 92.5, 73.8, 65.2, 64.6, 56.9, 56.0, 48.6, 45.5, 39.9, 38.9, 19.5, 18.7 [c]
8f/9f	222, 156.5, 136.0, 129.0, 128.7, 126.5, 123.8, 123.5, 122.9, 120.9, 120.3, 112.5, 111.9, 111.5, 91.2, 91.0, 73.9, 63.7, 63.2, 59.8, 57.0, 56.2, 42.8, 40.1, 35.0, 10.4, 10.3
10a/11a	222, 139.4, 138.9, 128.4, 126.6, 125.3, 125.2, 124.5, 123.1, 122.7, 122.5, 122.0, 121.8, 94.8, 94.1, 79.6, 77.2, 70.2, 70.1, 68.2, 68.1, 51.9, 50.4, 29.8, 27.0
10b/11b	223, 146.1, 145.6, 141.6, 139.8, 139.0, 135.9, 129.9, 129.0, 128.7, 127.5, 127.4, 127.0, 126.7, 125.9, 125.5, 124.6, 123.0, 122.8, 121.9, 121.8, 119.1, 115.6, 93.0, 92.4, 84.1, 70.7, 70.3, 68.2, 57.4, 56.9, 45.9, 43.2, 32.0, 25.3
10c/11c	222, 140.5, 139.8, 139.1, 138.5, 132.8, 132.1, 131.9, 129.4, 129.0, 128.8, 128.5, 127.7, 126.9, 125.7, 125.3, 124.6, 123.6, 123.1, 122.9, 122.7, 122.0, 121.9, 121.8, 119.0, 93.3, 93.2, 92.6, 91.4, 81.4, 80.8, 71.4, 69.5, 53.2, 53.0, 31.9, 30.0, 29.1, 29.0, 1.3, 1.2
10d/11d	223, 142.0, 139.8, 138.9, 138.7, 137.4, 135.0, 129.5, 129.4, 129.2, 128.6, 128.4, 128.0, 127.8, 126.5, 126.4, 126.1, 125.3, 125.1, 123.4, 122.7, 122.3, 121.5, 118.7, 106.8, 95.4, 93.4, 92.6, 83.6, 72.?, 70.7, 68.7, 54.7, 54.0, 47.5, 47.1, 42.9, 40.4, 38.1
12a	222, 150.2, 133.2, 129.2, 128.1, 123.9, 116.7, 94.4, 68.4, 55.2, 49.9, 36.8, 32.5, 29.2 [b]
12b	222, 150.6, 149.9, 147.3, 144.2, 129.2, 128.8, 128.1, 127.6, 126.2, 125.4, 124.3, 116.6, 92.6, 82.8, 68.0, 62.1, 57.0, 48.4, 28.0 [b]
12c	222, 150.2, 133.2, 132.1, 129.6, 128.7, 128.4, 128.3, 124.2, 123.1, 119.2, 116.9, 93.0, 91.3, 80.6, 69.4, 58.8, 52.3, 34.4, 29.9, 27.9, 1.2 [b]
12d/13d	222, 150.3, 137.7, 133.0, 129.8, 129.7, 129.4, 128.8, 128.7, 128.6, 128.4, 128.3, 128.2, 126.6, 126.4, 126.2, 124.6, 124.3, 124.0, 119.3, 117.5, 117.4, 116.8, 92.4, 92.1, 71.4, 68.9, 60.8, 57.5, 53.9, 53.3, 49.3, 46.0, 45.7, 44.9, 43.8, 40.1, 38.1, 28.5, 28.1
12e/13e	223, 150.8, 150.4, 129.3, 128.8, 128.5, 128.1, 124.4, 124.1, 123.9, 119.4, 117.4, 116.7, 92.8, 91.9, 91.6, 71.6, 68.6, 61.1, 57.5, 52.6, 52.0, 49.3, 48.3, 45.3, 43.2, 39.7, 38.0, 36.1, 29.0, 19.4, 18.3, 17.8

[a] All spectra in $CDCl_3$ except as noted. [b] Major isomer peaks only. [c] In CD_3COCD_3.

trum. In each case, the protons identified as H(1)–H(4) in **8**, **10** and **12** or H(1')–H(4') in products **9**, **11** and **13** formed adjacent sets, as indicated by couplings of ca. 6 Hz. Identification of C(1) attack in the major isomer required the solution of a crystallographic structure for hydride adduct **8a** (vide infra). The relative chemical shifts for the major and minor isomers of each product were then compared with those established for **8a** and **9a**. Proton resonances for H(4) and H(1') were least influenced by the attached group and were invariably found in the same relative positions.

^{1}H NMR also revealed that nucleophile addition had occurred in a stereospecifically exo fashion, i.e. on the opposite face of the ring system from that occupied by manganese. This was indicated by the moderate coupling ($J \approx 6$ Hz) of H(1) to H(2) in **8**, **10** and **12** and H(3') to H(4') in **9**, **11** and **13**. Such coupling is diagnostic of H(1) and H(4') being in the endo position. For the hydride adducts, H(1-exo) and H(4'-exo) were also present. These resonances were coupled respectively only to H(1-endo) and H(4'-endo) with $J \approx 12$ Hz. A lack of coupling between the H(1-exo) and H(2) would be expected based on the torsion angle H(1B)–C(1)–C(2)–H(2A) of ca. 90° found in the X-ray structure of **8a**. Use of $NaBD_4$ in the reaction led to the absence of this exo proton signal in the ^{1}H NMR spectrum. The cyclohexadienyl rings were easily cleaved from complexes **8**–**13** using the Jones reagent [4]. Under these oxidizing and acidic conditions, the ring underwent rearomatization, yielding C(1)- and C(4)-substituted DBF, DBT and XAN compounds.

2.2. Solvolysis kinetics of 5–7

The kinetics of **5** and **6** reacting with CH_3CN at 25.0 ± 0.2 °C under pseudo first-order conditions were measured by IR spectroscopy at several CH_3CN concentrations (diluted using CH_2Cl_2). A small amount of ferrocenium ion was added to each solution. This served to remove trace reductants which are known to catalyze ligand substitution in $[(\eta^6\text{-arene})Mn(CO)_3]^+$ [15]. Experimental values for k_{obs} and for second-order k are presented in Table 7. Complexes **5** and **6** behave similarly, showing average k values of $4.6 \pm 0.6 \times 10^{-5}$ M^{-1} s^{-1} and $4.4 \pm 1.0 \times 10^{-5}$ M^{-1} s^{-1} respectively. Complex **7** underwent solvolysis at a much slower rate, requiring the use of neat CH_3CN at 60 °C

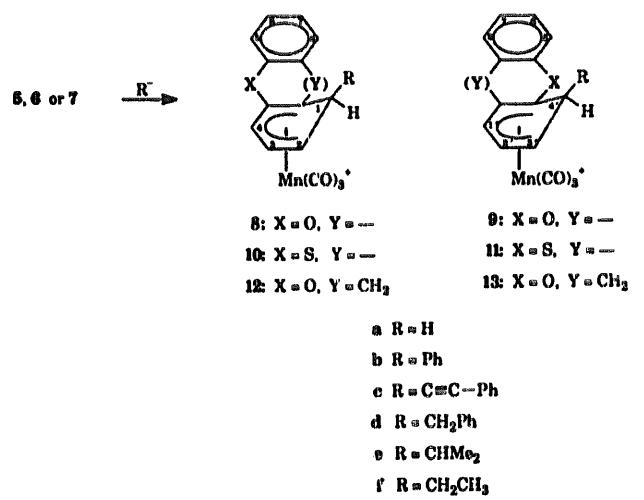

8: X = O, Y = —
10: X = S, Y = —
12: X = O, Y = CH_2

9: X = O, Y = —
11: X = S, Y = —
13: X = O, Y = CH_2

a R = H
b R = Ph
c R = C≡C–Ph
d R = CH_2Ph
e R = $CHMe_2$
f R = CH_2CH_3

Scheme 2.

Table 7
Kinetics results for arene displacement from complexes **5**–**7** by acetonitrile

Complex	T (°C)	$[CH_3CN]$ (M)	k_{obs} ($s^{-1} \times 10^4$)	k ($M^{-1}s^{-1} \times 10^5$)
5	25	10.1	4.8	4.8
5	25	5.0	2.0	3.9
5	25	2.6	1.32	5.2
5	25	1.0	0.44	4.4
6	25	10.1	3.3	3.3
6	25	5.0	2.0	3.9
6	25	2.6	1.43	5.6
6	25	1.1	0.46	4.6
7	60	19.1	1.9	1.0

Table 8
Crystal data and structure refinement for **8a**

Empirical formula	$C_{15}H_9MnO_4$
Formula weight	308.16
Temperature (K)	298(2)
Wavelength (Å)	0.71073
Crystal system	monoclinic
Space group	$P2_1/c$
Unit cell dimensions	
a (Å)	15.301(2)
b (Å)	6.4422(12)
c (Å)	12.988(2)
β (deg)	90.888(13)
Volume (Å^3)	1280.1(3)
Z	4
Density (calc) (Mg m^{-3})	1.599
Absorption coefficient (mm^{-1})	1.040
F(000)	624
Crystal size (mm^3)	0.32 × 0.41 × 0.62
θ range for data collection (deg)	2.66 to 30.00
Index ranges	$-21 \le h \le 21, -9 \le k \le 1, -1 \le l \le 18$
Reflections collected	4851
Independent reflections	3132 (R_{int} = 0.0340)
Refinement method	Full-matrix least squares on F^2
Data/restraints/parameters	3732/0/181
Goodness-of-fit	0.918
Final R indices ($I > 2\sigma(I)$)	$R1$ = 0.0410, $wR2$ = 0.0945
R indices (all data)	$R1$ = 0.0705, $wR2$ = 0.1040
Largest difference peak and hole (e Å^{-3})	0.398 and −0.252

Table 9
Atomic coordinates ($\times 10^4$) and equivalent isotropic displacement parameters U_{eq} ($Å^2 \times 10^3$) [a] for **8a**

Atom	x	y	z	U_{eq}
Mn(1)	1616(1)	1329(1)	3891(1)	37(1)
O(1)	3614(1)	974(3)	7513(2)	78(1)
O(2)	593(1)	−1401(4)	7513(2)	78(1)
O(3)	1948(1)	1816(3)	10488(1)	66(1)
O(4)	109(1)	2688(3)	10096(2)	88(1)
C(1)	2420(2)	2047(4)	7043(2)	52(1)
C(2)	1738(2)	3389(4)	7544(2)	54(1)
C(3)	1904(2)	4436(4)	8456(2)	54(1)
C(4)	2541(2)	3722(4)	9170(2)	49(1)
C(5)	3012(1)	1979(4)	8847(2)	42(1)
C(6)	3850(1)	−789(4)	8918(2)	46(1)
C(7)	4450(1)	−2218(5)	9254(2)	60(1)
C(8)	4631(2)	−3807(5)	8585(3)	71(1)
C(9)	4227(2)	−3944(5)	7629(3)	68(1)
C(10)	3609(2)	−2504(4)	7307(2)	56(1)
C(11)	3414(1)	−885(4)	7969(2)	44(1)
C(12)	2845(1)	927(4)	7927(2)	41(1)
C(13)	988(1)	−362(4)	8062(2)	49(1)
C(14)	1816(1)	−582(4)	9874(2)	42(1)
C(15)	688(2)	2194(4)	9610(2)	54(1)

[a] Equivalent isotropic U defined as one-third of the trace of the orthogonalized U_{ij} tensor.

to achieve a reasonable rate of reaction. Under these conditions, k was measured at 1.0×10^{-5} M^{-1} s^{-1}.

2.3. Molecular structure of 8a

An X-ray structural analysis was carried out to aid in the confirmation of regioselective C(1) attack on **5**–**7**. Suitable crystals of the hydride adduct **8a** were grown by cooling a concentrated hexane solution of this complex. Large orange crystals were obtained. After cutting, several fragments were found to exhibit twinning. However, a second cutting of one crystal provided a single crystal fragment. Solution of the monoclinic structure was accomplished by direct methods. Crystallographic data are listed in Table 8, fractional non-hydrogen atom coordinates in Table 9, and selected bond lengths and angles in Table 10. A thermal ellipsoid drawing is shown in Fig. 1. The relative positions of the saturated carbon C(1) and oxygen O(1) confirmed C(1) attack as predominant. The overall configuration of the complex is that of a piano stool with a carbonyl being roughly eclipsed under the saturated carbon in the dienyl system (C(1)). This results in eclipsing of carbonyl C(14)–O(3) under C(5) and O(1). All three carbonyls are roughly linear. An approximate plane is formed by C(2)–C(12) and O(1). However, least squares analysis revealed that the cyclohexadienyl ring plane forms an angle of about 5° with respect to the rest of the unsaturated ring system. The plane formed by dienyl carbons C(2)–C(5) and C(12) is inclined slightly in the direction of the metal atom. As is typical of a cyclohexadienyl complex,

Table 10
Selected bond lengths (Å) and angles (deg) in **8a**

Mn(1)–C(14)	1.797(2)	Mn(1)–C(13)	1.799(3)
Mn(1)–C(15)	1.801(2)	Mn(1)–C(4)	2.121(2)
Mn(1)–C(3)	2.128(2)	Mn(1)–C(5)	2.178(2)
Mn(1)–C(2)	2.206(2)	Mn(1)–C(12)	2.289(2)
O(1)–C(5)	1.376(3)	O(1)–C(6)	1.391(3)
O(2)–C(13)	1.144(3)	O(3)–C(14)	1.142(3)
O(4)–C(15)	1.141(3)	C(1)–C(12)	1.497(3)
C(1)–C(2)	1.511(3)	C(2)–C(3)	1.383(3)
C(3)–C(4)	1.412(3)	C(4)–C(5)	1.402(3)
C(5)–C(12)	1.393(3)	C(6)–C(7)	1.368(3)
C(6)–C(11)	1.394(3)	C(7)–C(8)	1.374(4)
C(8)–C(9)	1.382(4)	C(9)–C(10)	1.385(4)
C(10)–C(11)	1.387(3)	C(11)–C(12)	1.456(3)
C(14)–Mn(1)–C(13)	95.41(11)	C(14)–Mn(1)–C(15)	88.30(11)
C(13)–Mn(1)–C(15)	94.56(11)	C(14)–Mn(1)–C(4)	105.69(10)
C(13)–Mn(1)–C(4)	153.08(10)	C(15)–Mn(1)–C(4)	102.45(11)
C(14)–Mn(1)–C(3)	143.08(10)	C(13)–Mn(1)–C(3)	121.43(10)
C(15)–Mn(1)–C(3)	90.83(10)	C(4)–Mn(1)–C(3)	38.83(9)
C(14)–Mn(1)–C(5)	89.66(9)	C(13)–Mn(1)–C(5)	128.02(9)
C(15)–Mn(1)–C(5)	137.35(11)	C(4)–Mn(1)–C(5)	38.04(9)
C(3)–Mn(1)–C(5)	66.73(9)	C(14)–Mn(1)–C(2)	163.82(9)
C(13)–Mn(1)–C(2)	86.59(10)	C(15)–Mn(1)–C(2)	107.59(11)
C(4)–Mn(1)–C(2)	68.53(9)	C(3)–Mn(1)–C(2)	37.17(9)
C(5)–Mn(1)–C(2)	76.62(9)	C(14)–Mn(1)–C(12)	100.29(9)
C(13)–Mn(1)–C(12)	92.33(9)	C(15)–Mn(1)–C(12)	168.44(10)
C(4)–Mn(1)–C(12)	67.91(8)	C(3)–Mn(1)–C(12)	77.65(9)
C(5)–Mn(1)–C(12)	36.23(8)	C(2)–Mn(1)–C(12)	63.55(9)
C(5)–O(1)–C(6)	105.1(2)	C(12)–C(1)–C(2)	103.9(2)
C(3)–C(2)–C(1)	121.9(2)	C(3)–C(2)–Mn(1)	68.34(13)
C(1)–C(2)–Mn(1)	93.7(2)	C(2)–C(3)–C(4)	121.3(2)
C(2)–C(3)–Mn(1)	74.49(14)	C(4)–C(3)–Mn(1)	70.32(14)
C(5)–C(4)–C(3)	114.6(2)	C(5)–C(4)–Mn(1)	73.19(13)
C(3)–C(4)–Mn(1)	70.85(14)	O(1)–C(5)–C(12)	112.6(2)
C(1)–C(5)–C(4)	122.9(2)	C(12)–C(5)–C(4)	124.0(2)
O(1)–C(5)–Mn(1)	122.8(2)	C(12)–C(5)–Mn(1)	76.26(12)
C(4)–C(5)–Mn(1)	68.78(13)	C(7)–C(6)–O(1)	124.3(2)
C(7)–C(6)–C(11)	124.3(2)	O(1)–C(6)–C(11)	111.4(2)
C(6)–C(7)–C(8)	116.1(3)	C(7)–C(8)–C(9)	121.6(3)
C(8)–C(9)–C(10)	121.5(3)	C(9)–C(10)–C(11)	118.0(3)
C(10)–C(11)–C(6)	118.4(2)	C(10)–C(11)–C(12)	135.6(2)
C(6)–C(11)–C(12)	105.9(2)	C(5)–C(12)–C(11)	104.9(2)
C(5)–C(12)–C(1)	119.7(2)	C(11)–C(12)–C(1)	131.8(2)
C(5)–C(12)–Mn(1)	67.51(11)	C(11)–C(12)–Mn(1)	124.5(2)
C(1)–C(12)–Mn(1)	90.83(13)	O(2)–C(13)–Mn(1)	178.1(2)
O(3)–C(14)–Mn(1)	179.0(2)	O(4)–C(15)–Mn(1)	177.3(2)

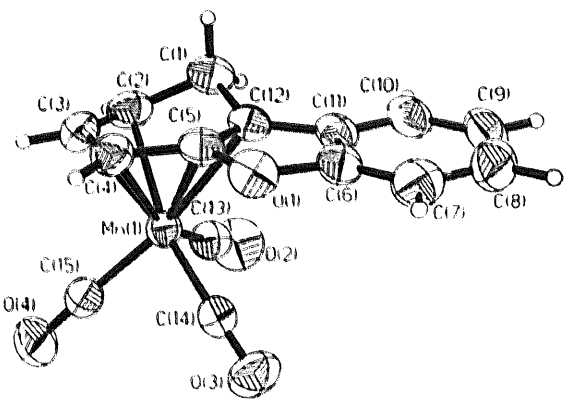

Fig. 1. Thermal ellipsoid drawing of $[(\eta^5\text{-}C_{12}H_9O)Mn(CO)_3]$, **8a** at the 50% probability level.

saturated carbon C(1) lies about 0.50 Å above the plane of the other ring carbons. The overall structure is quite similar to that of $[(\eta^5\text{-}C_{12}H_9O)Cr(CO)_3(SnPh_3)]$ which was produced by the addition of hydride to $[(\eta^6\text{-}DBF)Cr(CO)_3]$, followed by trapping of the resultant anion with Ph_3SnCl [16]. In the case of the chromium complex, strong C(1) preference for hydride attack was also noted.

3. Discussion

The $[Mn(CO)_3]^+$ complexes of DBF and DBT are highly reactive toward both neutral donor nucleophiles, such as acetonitrile, and toward anionic nucleophiles, such as hydride. The outcomes of these reactions are quite different, however. Whereas anions undergo addition to the coordinated arene to produce fused ring cyclohexadienyl complexes, neutral donors cause displacement of the aromatic ring.

The nucleophilic addition reactions of fused ring heterocyclic complexes show significant regioselectivity. Since the six-coordinated carbons of complexes **5–7** are chemically distinct, six isomeric products are theoretically possible. However, only two regioisomers were identified. The occurrence of C(1)-functionalization (**8, 10** and **12**) and C(4)-functionalization (**9, 11** and **13**) is consistent with the previously observed formation of **1** and **2** in the reactions of the (indole)manganese complexes and the formation of **3** and **4** in the reactions of the (benzofuran)manganese complex [8]. However, in the present case, a striking difference in regioselectivity is seen between addition to **5** and **7** vs. that to **6**. In the case of the DBT complex, **6**, there is a slight but consistent preference for attack at the C(1)-position. This selectivity disappears only when the bulky ^{i}Pr group is added. For the DBF and XAN complexes, **5** and **7**, nucleophiles which are stabilized through charge delocalization, BH_4^-, Ph^- and PhC_2^-, attack C(1) with 90% or greater selectivity. The highly stabilized anion of dimethyl malonate (sodium salt) was also found to give greater than 90% selectivity for C(1) attack on **5** and **7**; however, the products were difficult to fully purify. The C(1):C(4) regioselectivity sharply diminished with an decrease in carbanion stabilization from Ph^- to $PhCH_2^-$ to $CH_3CH_2^-$ and $(CH_3)_2CH^-$.

The high degree of regioselectivity encountered with DBF and XAN almost certainly results from the directing effect of the oxygen heteroatom. During addition reactions to the $[(\eta^6\text{-biphenyl})Mn(CO)_3]^+$, the phenyl substituent has been shown to exert very little directing effect toward nucleophilic attack [17]. Moreover, the anisole and phenyl ether complexes are known to be strongly *meta*-directing [3–5]. *Meta*-direction by electron-donating substituents can be rationalized using resonance arguments. A partial negative charge is developed on the *ortho*- and *para*-carbons through lone pair donation into the aromatic ring. This, of course, favors electrophilic substitution at these sites. For the same reason, this partial charge should disfavor nucleophilic attack at the *ortho* and *para* positions.

For the DBF, XAN and DBT complexes, six isomeric products are theoretically possible; however, addition to the ring junction positions can easily be ruled out on steric grounds. Attack at *ipso*-carbons is rarely observed; thus, for example, the pentamethylbenzene complex of $[Mn(CO)_3]^+$ is invariably attacked at the lone unsubstituted ring carbon [18]. Elimination of the fused positions leaves four remaining sites for addition to **5–7**. Relative to the heteroatom, two of these positions are *meta* (C(1) and C(3)), one is *ortho* (C(4)) and one is *para* (C(2)). The current results show that *meta* attack at C(1) is indeed found to predominate. Nevertheless, several questions arise:

1. Why is no attack seen at *meta* position C(3)?
2. What factors produce the varying regiochemical preference for attack at C(1)?
3. Why was no clear preference between products **3** and **4** encountered during previous study of the benzofuran complex?

With regard to the first question, it may be noted that all of the fused ring heterocycle complexes of $[Mn(CO)_3]^+$ examined thus far have demonstrated attack exclusively adjacent to ring junction carbons. In the present case, this effect even overrides the strong *meta*-directing effect of an oxygen substituent, favoring C(4) to C(3). The probable explanation involves the partial aromatic character of the fused heterocycle ring in **5–7**. The aromaticity of the central ring is increased upon ring slippage, leading to a small but significant contribution of **14**. η^4-Diene complexes typically add nucleophiles at the end of the coordinated system, yielding η^3-allyl products [19]. In the case of **14**, C(1) and C(4) represent the termini of an η^4-coordinated diene.

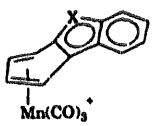

14

A trend toward 1:1 C(1):C(4) attack upon substrates **5–7** appears to occur with increasing nucleophile R group bulk. However, neither C(1) nor C(4) are hindered positions. Moreover, the less hindered ethyl Grignard yielded low regioselectivity, while the hindered dimethyl malonate anion gave rise to high regioselectivity. It should also be noted that steric arguements involving Grignard reagents are difficult to invoke given the associated nature of these species in solution [20]. The most probable origin for the observed regioselectivity

ity is an electronic effect. The most stabilized nucleophiles, BH_4^-, Ph^-, PhC_2^- and $(CH_3O_2C)_2CH^-$, produce the higher degrees of selectivity, in accordance with the reactivity–selectivity principal. The benzyl anion affords some selectivity, while the alkyl anions afford very little selectivity.

It is difficult to explain the very weak preference for *meta* addition previously encountered using the benzofuran complex [8]. Only two nucleophiles (Bu_4NBH_4 and LiMe) were reacted with this complex. Hydride is a mild donor and has shown high regioselectivity in the current study. However, the enhanced reactivity of the more soluble hydride salt may account for the lower regioselectivity observed in the previous work. In light of the new findings, it would be of interest to re-examine the reactions of $[(benzofuran)Mn(CO)_3]^+$.

It has previously been established that $[(\eta^6\text{-arene})Mn(CO)_3]^+$ complexes are subject to solvolysis by donor solvents according to Eq. (1) [21]. This reaction

$$[(\eta^6\text{-arene})Mn(CO)_3]^+ + 3\,\text{solvent} \rightarrow [Mn(\text{solvent})_3(CO)_3]^+ + \text{arene} \quad (1)$$

follows first-order kinetics in both the manganese complex and the donor molecule. Therefore, the reaction of Eq. (1) is most likely an associative process initiated by a ring slippage. We have recently published preliminary data showing that this solvolysis reaction is greatly accelerated for polycyclic aromatics over simple aromatics [9]. In the present study, the solvolysis kinetics of complexes **5** and **6** have been found to be identical within experimental error, showing average k values of $4.6 \pm 0.6 \times 10^{-5}\ M^{-1}\ s^{-1}$ and $4.4 \pm 1.0 \times 10^{-5}\ M^{-1}\ s^{-1}$ respectively. These data may be compared with the k value of $3.2 \times 10^{-9}\ M^{-1}\ s^{-1}$ for the toluene complex at 25 °C (calculated from data measured at 72.2 °C) [21]. Ring slippage of **5** or **6** to produce **14** will be greatly facilitated over the slippage of a simple aromatic ligand due to the incipient aromaticity of the fused heterocyclic ring. The heterocyclic ring in xanthene is not aromatic but is conjugated through a lone pair on the oxygen atom. The ease of ring slippage will therefore be expected to follow the trend: DBF, DBT > XAN ≫ toluene. Complex **7** yielded a k value of $1.0 \times 10^{-5}\ M^{-1}\ s^{-1}$ at 60 °C, confirming the expected trend. The greatly enhanced reactivity of complexes **5** and **6** toward solvolysis supports the ring slip mechanism.

Coordination, nucleophilic attack and decomplexation of these heterocycles constitute an overall nucleophilic aromatic substitution. The high regioselectivity for C(1) is especially significant, since no other general route exists for functionalization of this position. For all three fused heterocycles, electrophilic aromatic substitution leads to functionalization at C(2). (Under forcing conditions, C(7) is also attacked.) Nucleophilic aromatic substitution may be carried out on the xanthylium cation; but this leads to exclusive C(9) substitution. The work herein represents a versatile and general route to the otherwise inaccessible C(1) site in these compounds. Common nucleophiles can be used and regioselectivity is often high when the heteroatom is oxygen.

4. Experimental

4.1. General

All reactions were carried out under N_2 and solvents were dried by standard procedures. Tetrahydrofuran, diethyl ether or alkane solutions of organolithium and -magnesium reagents were used as supplied by Aldrich (Milwaukee, WI) with the exception of $MgBrCH_2Ph$ which was prepared by standard methods from $PhCH_2Br$ in diethyl ether. Infrared spectra were recorded on a Perkin–Elmer series 1600 FTIR using a liquid cell with CaF_2 windows, and ^1H and ^{13}C NMR spectra were collected using a General Electric QE-300 spectrometer. Microanalyses were carried out by Galbraith Laboratories, Knoxville, TN or Atlantic Microlab, Inc., Norcross, GA.

4.2. Synthesis of 5–7

The $[(arene)Mn(CO)_3]^+$ complexes were prepared by published methods [9]. Analytical data: **5**(BF_4) 76% (TFAA method) m.p. 119 °C (decomp.). Anal. Found: C, 45.4; H, 2.02. $C_{15}H_8BF_4MnO_4$. Calc.: C, 45.7; H, 2.05%. IR (CH_2Cl_2, cm^{-1}): ν(C≡O) 2079, 2020. ^1H NMR (CD_3COCD_3) (δ): 8.53 (d, 1 H, J = 7.8 Hz, H(4)), 8.17 (d, 1 H, J = 6.6 Hz, H(5)), 7.93 (m, 2 H, H(1,2)), 7.70 (t, 1 H, J = 6.9 Hz, H(3)), 7.68 (d, 1 H, J = 7.0 Hz, H(8)), [illegible] (t, 1 H, J = 6.6 Hz, H(7)), 6.66 (t, 1 H, J = 6.2 Hz, H(6)); $^{13}C\{^1H\}$ NMR (CD_3COCD_3) (δ): 216 (CO), 160.5, 139.5, 133.9, 128.3, 121.8, 120.8, 114.2, 100.8, 100.3, 96.9, 94.0, 86.8. **6**(BF_4) 89% (TFAA method), analytical data previously reported [9]. **7**(PF_6) 60% (Fischer–Hafner method) m.p. 117 °C (decomp.). Anal. Found: C, 41.1; H, 2.21. $C_{16}H_{10}PF_6MnO_4$. Calc.: C, 41.2; H, 2.17%. IR (CH_2Cl_2, cm^{-1}): ν(C≡O) 2079, 2021. ^1H NMR (CD_3COCD_3) (δ): 7.44 (m, 2 H, H(2,3)), 7.36 (d, 1 H, J = 7.5 Hz, H(4)), 7.26 (d, 1 H, J = 7.9 Hz, H(5)), 7.21 (d, 1 H, J = 6.2 Hz, H(1)), 7.10 (t, 1 H, J = 6.2 Hz, H(7)), 6.81 (d, 1 H, J = 6.6 Hz, H(8)), 6.52 (t, 1 H, J = 6.2 Hz, H(6)); $^{13}C\{^1H\}$ NMR (CD_3COCD_3) (δ): 216 (CO), 160.5, 139.5, 133.9, 128.3, 121.8, 120.8, 114.2, 100.8, 100.3, 96.9, 94.0, 86.8.

4.3. Nucleophile addition reactions

Arene complex **5**, **6** or **7** (0.5–1 mmol) was dissolved or suspended in solvent (tetrahydrofuran, diethyl ether

or CH_2Cl_2, 20–40 ml) at room temperature, 0 or −78 °C under N_2. The nucleophile solution (2–12 mmol) was then added dropwise by syringe with stirring. The progress of the reaction was monitored by IR. Upon completion of the reaction, the solvent was removed in vacuo and the residue taken into diethyl ether and filtered through Al_2O_3. Grignard reactions were quenched with water and then dried over anhydrous $MgSO_4$. The ether was removed under a stream of nitrogen, leaving an oil or a solid. Representative syntheses are given below.

4.4. Preparation of 8a / 9a

To a stirred solution of **5** in 40 ml THF at room temperature (0.352 g, 0.893 mmol) was added $NaBH_4$ (0.0841 g, 2.22 mmol). After 1 h, the yellow solution color was unchanged, but IR indicated completion of the reaction. After the solvent was removed in vacuo, the oily residue was taken into diethyl ether and filtered through a small amount of Al_2O_3. The ether was removed under a stream of N_2 and the yellow, crystalline product was dried in vacuo. Yield (both isomers): 0.232 g, 93%.

4.5. Preparation of 10b / 11b

Grignard reagent MgBrPh (4 ml of 3 M solution in diethyl ether) was added via syringe to a stirred suspension of **6** (0.309 g, 0.752 mmol) in 40 ml diethyl ether at 0 °C. After about 10 min, a yellow solution had formed. IR indicated that the reaction had occurred. After warming to room temperature, about 2 ml H_2O were added. The organic layer was dried over anhydrous $MgSO_4$ for 1 h and then filtered through Al_2O_3. The ether was removed under a stream of N_2 and the yellow, oily product was dried under vacuum. Yield (both isomers): 0.301 g, 77%.

4.6. Preparation of 10c / 11c

To a stirred suspension of **6** (0.284, 0.721 mmol) in 40 ml diethyl ether at −78 °C was added LiC_2Ph (2 ml of 1 M solution in THF). After 2 h, a clear, brown solution had formed and the IR indicated that the reaction had occurred. The mixture was warmed to room temperature and the solvent was removed under vacuum. The brown, oily residue was chromatographed on Al_2O_3 with hexane–diethyl ether. After elution of a small amount of $[Mn_2(CO)_{10}]$, the product eluted. Evaporation and vacuum drying left a brownish, oily product. Yield (both isomers): 0.219 g, 72%.

4.7. Kinetic studies

Solvolysis reactions were carried out under pseudo first-order conditions by dissolving complex **5**, **6** or **7** (1.5 mM) and $[Cp_2Fe]PF_6$ (0.6 mM) into a solution of CH_3CN in CH_2Cl_2 which was pre-equilibrated to 25.0 ± 0.2 °C or 60.0 ± 0.2 °C in a Fisher Isotemp Model 910 thermo tatic bath. Samples were periodically withdrawn and immediately examined by IR spectroscopy. Absorbance values were measured for both reactant and product. The two sets of data produced roughly identical k_{obs} values.

4.8. X-ray diffraction study of 8a

Suitable crystals were grown by cooling a concentrated solution of **8a** in hexane at −6 °C. One of the large, block-shaped orange crystals was cut to the proper size and was glued to a glass fiber. X-ray data collection was carried out at 25 °C using a Siemens P4 single-crystal diffractometer (Mo Kα radiation, 0.71073 Å) controlled by XSCANS software. Omega scans were used for data collection, at variable speeds from 10 to 60° min^{-1}. Three standard reflections were measured after every 97 reflections; no systematic decrease in intensity was observed. Data reduction included profile fitting and an empirical absorption correction based on separate azimuthal scans for seven reflections (maximum and minimum transmission, 0.599 and 0.553). The structure was determined by direct methods and refined initially by use of programs in the SHELXTL 5.1 package, which were also used for all figures. All hydrogen atoms appeared in a difference map, and each was introduced in an ideal position, riding on the atom to which it is bonded. Each was refined with an isotropic temperature factor 20% greater than that of the ridden atom. All other atoms were refined with anisotropic thermal parameters. Final refinement on F^2 was carried out using SHELXL 93 [22]. Tables of thermal parameters, hydrogen atom coordinates and structure factors are available from the authors.

Acknowledgements

Acknowledgement is made to the Thomas F. and Kate Miller Jeffress Memorial Trust, the donors of the Petroleum Research Fund, administered by the American Chemical Society (PRF No. 26521-GB1), the Merck/AAAS Undergraduate Science Research Program and to the Thomas Llanso and Smokey Sherman Research Scholarship Program for support of this research. The X-ray equipment was purchased with assistance from an instrument grant from the National Science Foundation (CHE-8206423) and a grant from the National Institutes of Health (RR-06462).

References

[1] (a) M.F. Semmelhack, in E.W. Abel, F.G.A. Stone and G. Wilkinson (eds.), *Comprehensive Organometallic Chemistry II*, Vol. 12, Elsevier, Tarrytown, NY, 1995, p. 979; (b) L.A.P.

Kane-Maguire, E.D. Honig and D.A. Sweigart, *Chem. Rev.*, *84* (1984) 525.
[2] (a) R.D. Pike and D.A. Sweigart, *Synlett.*, (1990) 563; (b) T.-Y. Lee, Y.K. Kang, Y.K. Chung, R.D. Pike and D.A. Sweigart, *Inorg. Chim. Acta*, *214* (1993) 125.
[3] P.L. Pauson and J.A. Segal, *J. Chem. Soc. Dalton Trans.*, (1975) 1683.
[4] Y.K. Chung, P.G. Williard and D.A. Sweigart, *Organometallics*, *1* (1982) 1053.
[5] (a) E. Jeong and Y.K. Chung, *J. Organomet. Chem.*, *434* (1992) 225; (b) S.S. Lee, J.-S. Lee and Y.K. Chung, *Organometallics*, *12* (1993) 4640.
[6] (a) I.U. Khand, P.L. Pauson and W.E. Watts, *J. Chem. Soc. C*, (1968) 2257; (b) I.U. Khand, P.L. Pauson and W.E. Watts, *J. Chem. Soc. C*, (1968) 2261; (c) I.U. Khand, P.L. Pauson and W.E. Watts, *J. Chem. Soc. C*, (1969) 116; (d) J.F. McGreer and W.E. Watts, *J. Organomet. Chem.*, *110* (1976) 103; (e) M.F. Semmelhack and G.R. Clark, *J. Am. Chem. Soc.*, *99* (1977) 1675; (f) M.F. Semmelhack, G.R. Clark, R. Farina and M. Saeman, *J. Am. Chem. Soc.*, *101* (1979) 217; (g) R.G. Sutherland, R.L. Chowdhury, A. Piórko and C.C. Lee, *Can. J. Chem.*, *64* (1986) 2031; (h) R.G. Sutherland, C.H. Zhang, R.L. Chowdhury, A. Piórko and C.C. Lee, *J. Organomet. Chem.*, *333* (1987) 367; (i) C.H. Zhang, R.L. Chowdhury, A. Piórko, C.C. Lee and R.G. Sutherland, *J. Organomet. Chem.*, *346* (1988) 67.
[7] (a) W.H. Miles, P.M. Smiley and H.R. Brinkman, *J. Chem. Soc. Chem. Commun.*, (1989) 1897; (b) W.H. Miles, and H.R. Brinkman, *Tetrahedron Lett.*, *33* (1992) 589; (c) G.R. Krow, W.H. Miles, P.M. Smiley, W.S. Lester and Y.J. Kim, *J. Org. Chem.*, *57* (1992) 4040.
[8] W.J. Ryan, P.E. Peterson, Y. Cao, P.G. Williard, D.A. Sweigart, C.D. Baer, C.F. Thompson, Y.K. Chung and T.-M. Chung, *Inorg. Chim. Acta*, *211* (1993) 1.
[9] S. Sun, L.K. Yeung, D.A. Sweigart, T.-Y. Lee, S.S. Lee, Y.K. Chung, S.R. Switzer and R.D. Pike, *Organometallics*, *14* (1995) 2613.
[10] J.D. Jackson, S.J. Villa, D.S. Bacon, R.D. Pike and G.B. Carpenter, *Organometallics*, *13* (1994) 3972.
[11] E.O. Fischer, H.A. Goodwin, C.G. Kreiter, H.D. Simmons, Jr., K. Sonogashira and S.B. Wild, *J. Organomet. Chem.*, *14* (1968) 359.
[12] C.C. Lee, B.R. Steele and R.G. Sutherland, *J. Organomet. Chem.*, *186* (1980) 265.
[13] J.W. Hachgenei and R.J. Angelici, *Organometallics*, *8* (1989) 14.
[14] J.R. Polam and L.C. Porter, *Organometallics*, *12* (1993) 3504.
[15] C.C. Neto, C.D. Baer, Y.K. Chung and D.A. Sweigart, *J. Chem. Soc. Chem. Commun.*, (1993) 816.
[16] J.-P. Djukic, F. Rose-Munch, F. Rose and Y. Dromzee, *J. Am. Chem. Soc.*, *115* (1993) 6434.
[17] J.P. Gutheil and R.D. Pike, unpublished work.
[18] R.D. Pike, T.J. Alavosus, C.A. Camainoi-Neto, J.C. Williams, Jr. and D.A. Sweigart, *Organometallics*, *8* (1989) 2631.
[19] K.F. McDaniel, in E.W. Abel, F.G.A. Stone and G. Wilkinson (eds.), *Comprehensive Organometallic Chemistry II*, Vol. 12, Elsevier, Tarrytown, NY, 1995, p. 601.
[20] (a) E.C. Ashby and F. Walker, *J. Organomet. Chem.*, *7* (1967) P17; (b) F.W. Walker and E.C. Ashby, *J. Am. Chem. Soc.*, *91* (1969) 3845.
[21] L.A.P. Kane-Maguire and D.A. Sweigart, *Inorg. Chem.*, *18* (1979) 700.
[22] G.M. Sheldrick, *J. Appl. Crystallogr.*, in preparation.